Final Report:	Unoccupied Aerial Vehicle (UAV)-Based Monitoring of the Spatial and Temporal Dynamics of Dredged Material Used to Restore Crab Bank in Charleston Harbor, South Carolina.

Principal Investigator:	Dr. Peter Kingsley-Smith, Senior Marine Scientist, Shellfish Research Section, Marine Resources Research Institute, South Carolina Department of Natural Resources
Co-Principal Investigators:	Dr. Denise Sanger, Senior Marine Scientist, SCDNR MRRI Gary Sundin, Wildlife Biologist III, SCDNR MRRI
Collaborators:	Dr. Andrew Tweel, Assistant Marine Scientist., SCDNR MRRI Graham Wagner, Wildlife Biologist II, SCDNR MRRI Lauren Faulk, Wildlife Biologist I, SCDNR MRRI Greg Rothman, Wildlife Biologist I, SCDNR MRRI Pamela Marcum, Wildlife Biologist III, SCDNR MRRI Norm Shea, Wildlife Biologist II, SCDNR MRRI Joseph Cowan, Wildlife Biologist II, SCDNR MRRI

Period of Performance:	October 1, 2020 – December 31, 2022

Aerial photograph of Crab Bank, taken by SCDNR Shellfish Research Section, March 14, 2022.

Background

Crab Bank, on the eastern side of Charleston Harbor, Charleston, South Carolina, was used as nesting habitat for shorebirds from the 1950s through 2017 (SCDNR, unpublished data). Due to erosion, the island decreased in size over the course of several decades, until impacts from Hurricane Irma in September 2017 removed the last areas of habitat with sufficient elevation to support shorebird nesting. As a result, nesting did not occur on the remaining vestiges of the island during the 2018 – 2021 nesting seasons. A decision was made to use a portion of the materials dredged from the Charleston Harbor as part of the Post-45 Deepening Project to restore a footprint of suitable nesting habitat at Crab Bank (Figure 1). Material placement was completed in November of 2021.

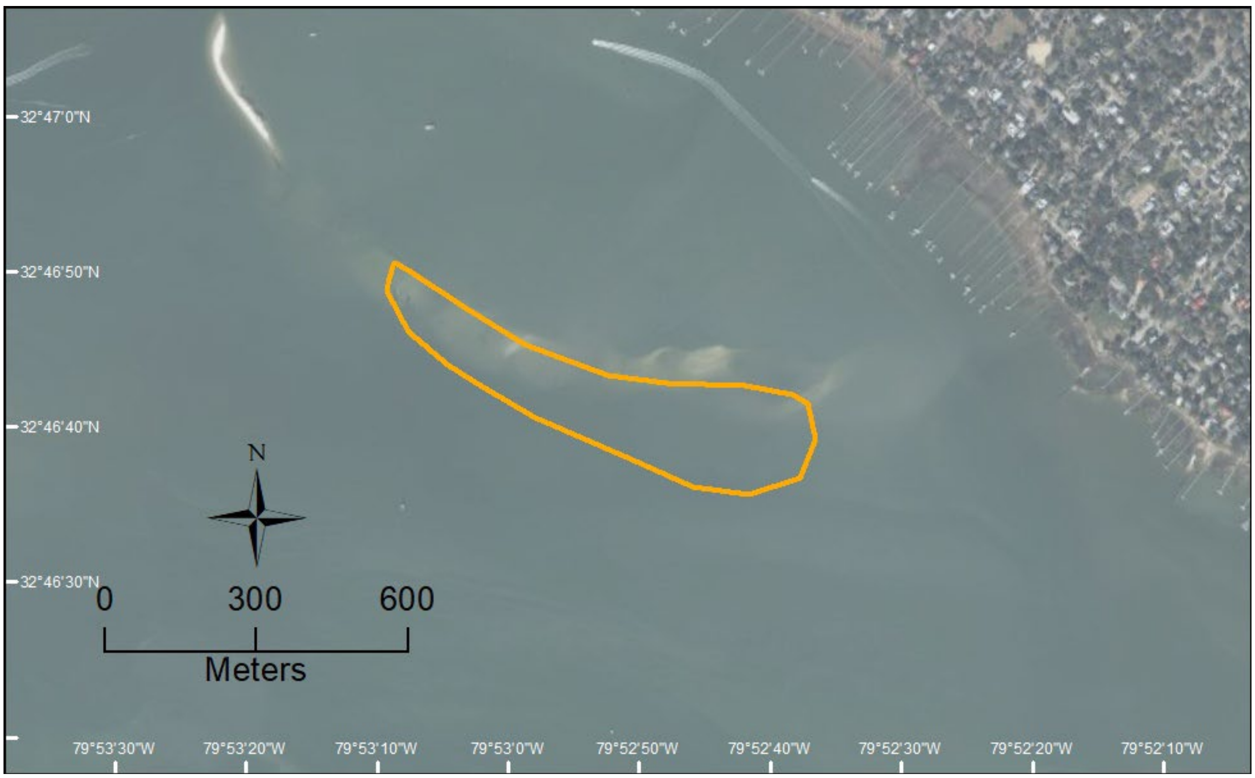

Figure 1. Planned footprint for a restored high-ground bird nesting area on Crab Bank, in Charleston Harbor, SC, shown over 2020 imagery indicating that the bank was primarily subtidal at this time.

Audubon South Carolina, with funding provided through the National Fish and Wildlife Foundation's National Coastal Resilience Fund (NFWF-NCRF), was tasked with monitoring the physical characteristics of Crab Bank post-construction. To this end, Audubon South Carolina contracted the South Carolina Department of Natural Resources (SCDNR) to complete physical monitoring of the new habitat to track changes in key geomorphological characteristics during the year immediately following the completion of material placement. SCDNR planned to complete the monitoring using a range of available expertise and equipment, but ultimately primarily used a small unoccupied aerial vehicle (UAV) to create a series of imagery and elevation maps that could be used to measure and analyze key metrics. This report summarizes the results of these efforts, as conducted from April 26, 2021 to December 19, 2022.

Executive Summary

Activities completed

SCDNR staff monitored key physical characteristics of Crab Bank over the course of 12site visits (Table 1). Pre-construction data were collected on April 26, 2021. The first post-construction dataset was collected on December 1, 2021, less than a month after the completion of material placement, establishing a post-construction baseline. Ten additional monitoring datasets were collected over the next year, approximately monthly, with the final dataset collected on December 19, 2022. All physical monitoring data were collected around low tides occurring between 9:00 am and 3:00 pm EST.

Monitoring events were scheduled approximately monthly, except during the bird nesting season, when visits were less frequent to minimize potential disturbance to nesting birds. SCDNR shorebird biologists were consulted prior to each physical monitoring visit, and all recommendations were carefully followed to avoid disturbing nesting birds. From April 2022 – September 2022, the high ground of the island was not accessed, to avoid disturbing nesting birds.

Table 1. List of monitoring events completed and data types collected by researchers at the South Carolina Department of Natural Resources as part of an effort measure changes in geomorphological characteristics of Crab Bank, Charleston Harbor, SC, following the re-construction of the island using dredged materials.

Date	Monitoring Type	UAV Flight	Sediment Collection	Elevation Transects
4/26/2021	Pre-construction	x	x	x
12/1/2021	Post-construction baseline	x	x	x
1/13/2022	Post-construction monitoring	x	x	x
2/14/2022	Post-construction monitoring	x	x	x
3/14/2022	Post-construction monitoring	x	x	x
4/25/2022	Post-construction monitoring	x		
5/26/2022	Post-construction monitoring	x		
7/25/2022	Post-construction monitoring	x		
9/7/2022	Post-construction monitoring	x		
10/10/2022	Post-construction monitoring	x	x	x
11/22/2022	Post-construction monitoring	x	x	x
12/19/2022	Post-construction monitoring	x	x	x

During each monitoring event, a small unoccupied aerial vehicle (UAV) was used to collect digital photos which were processed to create digital orthomosaic imagery (Figure 2) and a digital surface model (DSM) for use in GIS applications. In addition to UAV data, sediment samples were collected and GNSS elevation transects were completed on eight of the 12 monitoring visits. Sediment collection and transect profile data were not collected from April 2022 – September 2022 to avoid disturbing nesting shorebirds.

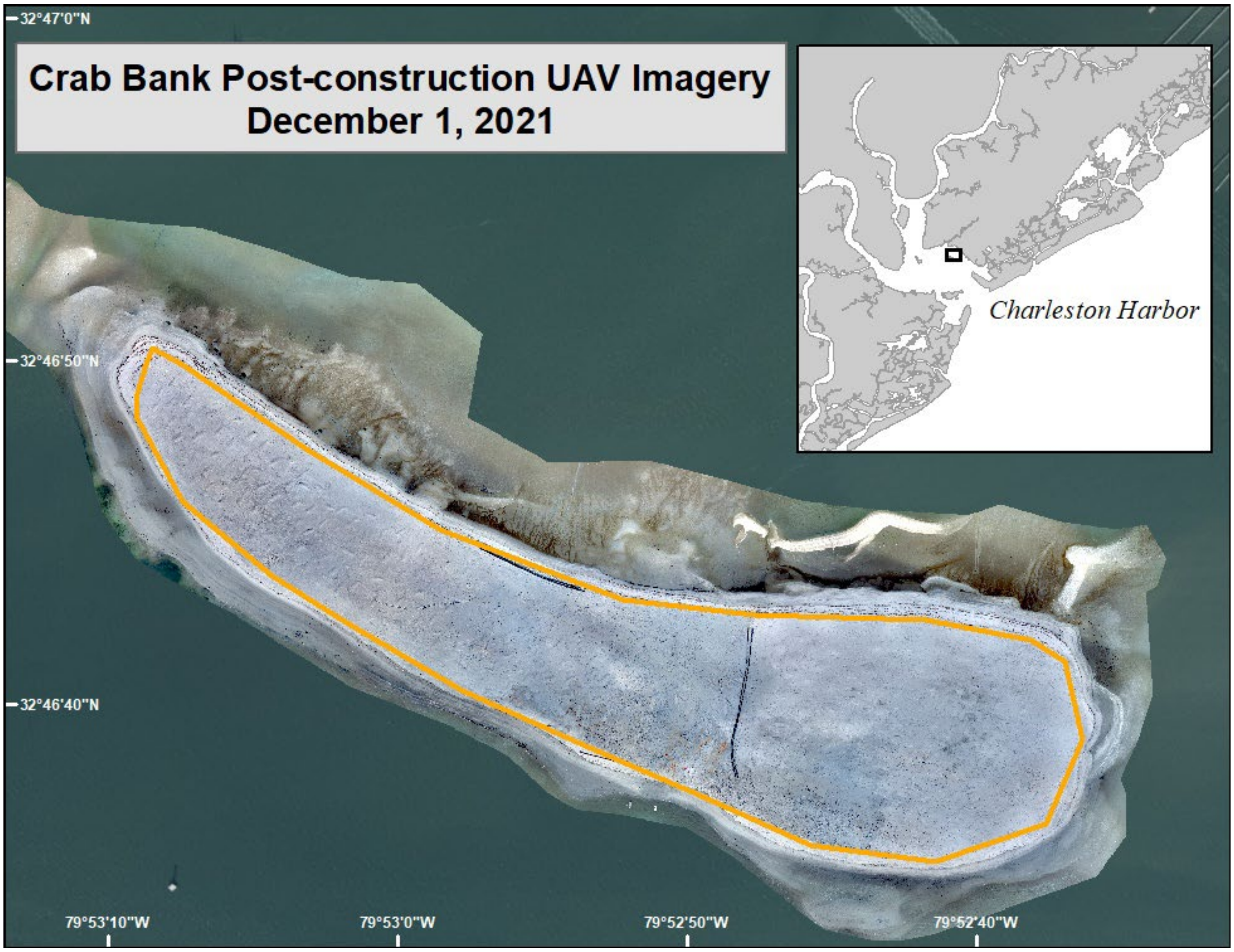

Figure 2. Example of UAV-derived orthomosaic imagery created from the initial post-construction monitoring event at Crab Bank, SC on December 1, 2021. The orange line indicates the pre-planned footprint.

UAV products

All UAV flights resulted in products useful for analyzing geomorphological changes to Crab Bank during the monitoring period. The resolution of the GIS products ranged from 1.2 – 1.9 cm/pixel (Table 2). The accuracy of the products, expressed in root mean square error (RMSE) ranged from 0.02 – 0.06 m horizontally and from 0.03 – 0.09 m vertically (Table 3).

Areal, volumetric, and elevational changes

The mean higher high water (MHHW) contour line, derived from UAV products for each post-construction visit, was used to estimate key physical characteristics of Crab Bank. The area contained within this contour polygon (referred to as "high ground" in this report), remained constant at around 16 hectares (39.5 acres) throughout the monitoring period (Table 4). The estimated volume within the MHHW contour fluctuated over the course of the post-construction monitoring period and there was a modest estimated net volume loss. The elevation of the interior of the island immediately post-construction primarily ranged from 0.5 – 1.5 m above MHHW (Figure 7). Over the post-construction monitoring period some high ground areas of Crab Bank experienced estimated elevation losses of up to 0.30 m (Figure 8). The southern border of the island experienced larger changes, primarily resulting from a gradual change from a relatively sinuous to a relatively straight configuration. Both losses and gains were observed on the southern border, but the overall net change was a loss of elevation. The western and eastern ends of the island gained elevation, suggesting that material from the southern border may have been re-deposited at the ends of the island by longshore tidal currents. An area near the center of the southern border was at risk of inundation at very high tides (Figure 9), and apparently experienced inundation in early November, 2022 (Figure 10). Some error is expected in UAV-derived estimates, warranting caution in interpreting the precise magnitude of these changes. Nevertheless, independent data strongly support the reality of elevation changes within this general range (Figures 12 & 13).

Shoreline change

With shoreline defined as the MHHW contour line, the shoreline on the southern border of Crab Bank showed a general erosional pattern, the west and east ends experienced accretion, and the northern border remained relatively stable (Figure 11 & Table 6). This is consistent with the findings of the elevation change analyses. The fastest erosion rate was observed on the southeastern border (Figure 11). Environmental variables including wind and tidal height performed poorly at explaining rates of shoreline change (Table 7), although the inclusion of other predictor variables or the use of different analytical approaches are likely to improve understanding of the relationship between environmental variables and physical changes on Crab Bank.

Sediment analysis

From a series of sediment samples collected following material placement, grain size patterns varied across the island. Increasing sand and calcium carbonate and decreasing silt/clay percentages indicated a gradual coarsening of material between the December 2021 and December 2022 sampling. (Table 8, Figures 14 -16). Samples collected in the center of the island remained relatively stable for all grain sizes throughout the study, relative to samples collected in the intertidal zones.

Methods

Unoccupied aerial vehicle flights

During each monitoring event, a DJI Phantom® 4 Pro V2 quadcopter unoccupied aerial vehicle (UAV) was used to collect aerial imagery of Crab Bank. Flights were planned and implemented using the DJI Ground Station Pro flight application. During each flight, a series of overlapping images was collected by flying a pre-planned grid pattern. Flight plans were repeated on subsequent visits to standardize data collection. All flights were conducted at altitudes between 47.2 meters and 68.6 meters above ground level. For each flight, visible ground control point (GCP) targets were deployed within the flight area. The locations of these targets, visible in the collected imagery, were recorded using a survey-grade Trimble R8 global navigation satellite system (GNSS). UAV images were processed using Pix4Dmapper photogrammetry software (v.4.8.1, Pix4D SA, Switzerland) to create digital imagery orthomosaics and digital surface models (DSM) that could be viewed and manipulated using GIS software. During processing, GCP location data were used to georectify the imagery and elevation products. Orthomosaics and DSMs were processed in the following projected horizontal coordinate system: NAD83 UTM Zone 17N. DSMs were referenced to the NAVD88 vertical datum using the GEOID 18 geoid model. During each visit in which monitoring staff entered the high ground area of the island, random GNSS point data were opportunistically collected to allow the estimation of vertical error associated with final GIS products.

To avoid disturbing nesting birds during the April – September period, nine semi-permanent GCPs were established on Crab Bank in February 2022 (Figure 3). Each GCP consisted of a bucket lid with a black and white target fixed to a 2-foot steel rebar pole driven into the substrate. These GCPs remained in place for the remainder of the monitoring period and were used to georectify the GIS products created from UAV flights. During the nesting period, SCDNR monitoring staff conducted all UAV activities from the shoreline or in a vessel anchored near the shoreline and did not place additional GCPs on the island. Following the nesting period, staff continued to use the permanent GCPs, but also deployed additional temporary GCPs for each flight.

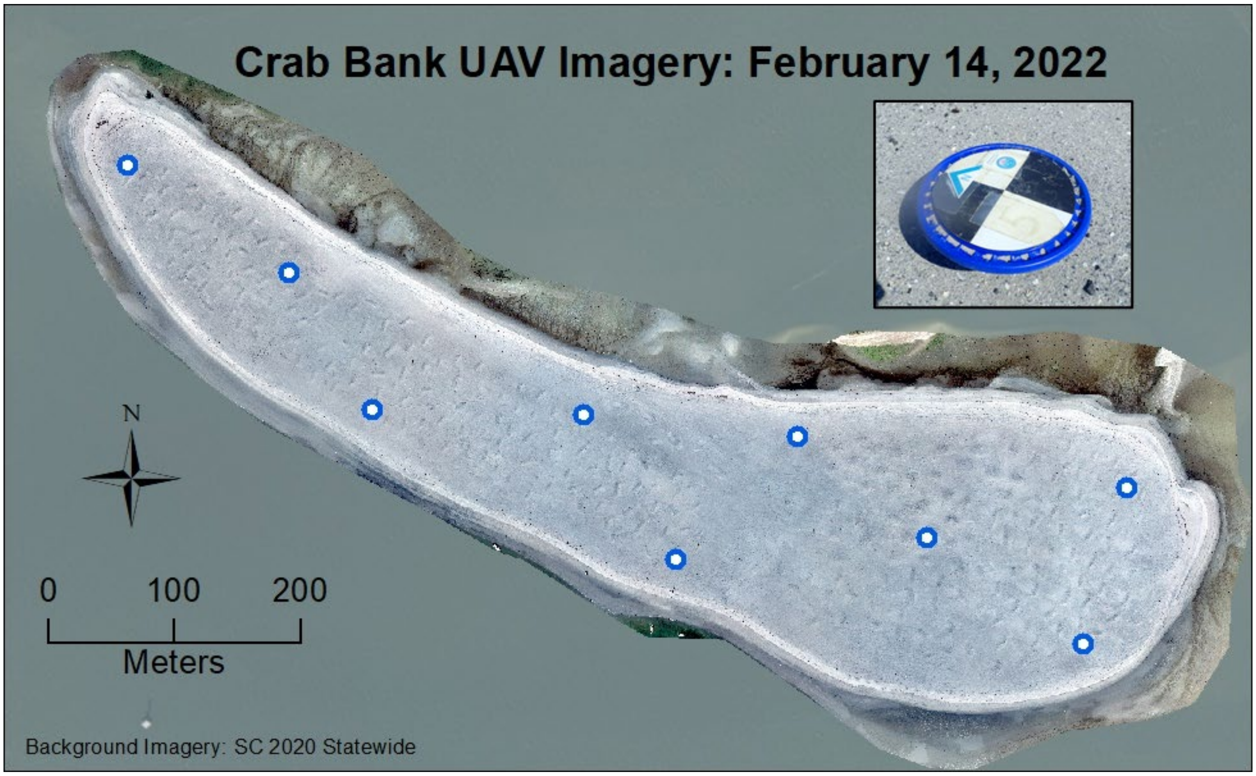

Figure 3. Location of nine permanent ground control points (detail inset) established on Crab Bank in February 2022.

Immediately prior to and following each monitoring visit, excluding visits during the bird nesting season, the GNSS units were checked in at a National Geodetic Survey (NGS) survey control benchmark (PID CJ0398) located approximately 3.2 km from Crab Bank on the Fort Johnson peninsula on James Island, SC. At least four check-in locations were recorded for each monitoring visit for each GNSS unit and the combined root mean square error (RMSE) was calculated from the horizontal and vertical differences between the observed and predicted values, where the predicted values were the horizontal position and elevation values reported by the NGS.

The horizontal and vertical RMSE of digital drone products (georectification error), created from data collected outside of the bird nesting season, was estimated from the differences between observed and predicted data collected with the GNSS units. Georectification error was not calculated during the bird nesting period (April – September) because SCDNR monitoring staff did not enter the interior of the island to record the necessary data. To estimate horizontal RMSE of the orthomosaics, several additional GCPs were placed and recorded with the GNSS but were not used in the georectification process. The locations of these GCPs were manually digitized from the processed orthomosaics (observed) and compared to the recorded GNSS location (predicted) to calculate RMSE. Vertical RMSE was calculated by using random GNSS points recorded from the monitoring area, as well as from points collected for transect profile measurements. Between 45 and 97 dispersed elevation points were collected with each visit. Because these data were independent of the georectification process, they were suitable for estimating RMSE. These points were used to extract the elevation data from the processed DSM (observed) which was compared to the recorded GNSS elevation value (predicted) to estimate vertical RMSE. Because of the greater effort required to place extra visual targets beyond those used for georectification, horizontal RMSE was necessarily estimated from fewer targets relative to the number of points used to calculate vertical RMSE.

Spatial analyses

ESRI GIS software (ArcGIS v.10.8.0, ESRI, Redlands, CA) was used to calculate key metrics from each monitoring visit. An elevation contour line was created representing the mean higher high water (MHHW) line from each DSM. The MHHW value was taken from NOAA Tide Station 8665530 (Charleston, SC) located approximately 3.6 km from Crab Bank within the same hydrologic system (Charleston Harbor). The MHHW datum at the location is 0.80 meters above 0.0 meters NAVD88 (1983 – 2001 epoch). Each MHHW contour line was used to create a single polygon and the area enclosed within the polygon was calculated. Changes in this area over time were used as a metric of habitat stability. The area enclosed within the MHHW contour polygons (*i.e.,* area of surface with elevations equal or above MHHW) were considered "high ground". Changes in distance across the MHHW polygon at established fixed transect locations were also calculated as a metric of habitat stability. Elevation data were visualized relative to the MHHW tidal datum and relative to observed water and potential water levels to assess inundation risk. A pixel-level elevation difference was calculated between DSMs for key periods of interest. The volume at each monitoring event and the change in volume between successive monitoring events was calculated from the DSM data.

Shoreline change analyses

Shoreline movements over the post-construction monitoring period were analyzed to determine rates of lateral shoreline change. Analyses were conducted using R (R Core Team, 2022), RStudio (RStudio Team, 2020), and AMBUR (Analyzing Moving Boundaries Using R, Jackson, 2018). The AMBUR package pairs with ESRI GIS software to use transects created at user-defined intervals to calculate change rates from digitized lines representing the position of the shoreline over time. The MHHW contour lines were used as the linear analysis features and transects were spaced at 10-meter intervals.

Endpoint change rates (EPR) were calculated as the total distance between two observed shoreline positions divided by the elapsed time between the observations. EPRs were calculated for each transect for each period (*i.e.,* periods between successive monitoring events). AMBUR also calculated weighted linear regression rates (WLR) at the transect level by performing linear regressions of change in distance over time. In this method, the slope of the regression line is equal to the WLR for the entire monitoring period (*i.e.,* period between the initial and final monitoring event). In weighted linear regression, each shoreline has a user-assigned accuracy value, and these values are used to weight the impact of the observations on the final solution and confidence estimates for model outputs. All analyses were conducted to provide 95% confidence values (α = 0.05) for estimates. The user-assigned accuracy was the combined value of the GNSS vertical RMSE and georectification RMSE for each monitoring event (previously described), and a penalty value of 0.25 m to account for un-estimated uncertainty.

During bird nesting season, when monitoring staff did not access the interior of the island and therefore did not collect data to directly estimate RMSE, alternative values were assigned to the shorelines generated from these visits. For vertical GNSS RMSE, a value of 0.20 meters was assigned; for georectification RMSE, the mean of values from the directly estimated flights was used. The large penalty error added to all shorelines and the large GNSS error added to the bird nesting flights were intended to make the confidence estimates from the AMBUR results conservative by exceeding any reasonable worst-case scenario and were based on experience from over 50 independent mapping flights for which SCDNR researchers have directly estimated error.

Environmental analyses

EPR values from the AMBUR output were used as response variables to investigate potential environmental explanations for shoreline change patterns on Crab Bank. Analyses were conducted using R (R Core Team, 2022), RStudio (RStudio Team, 2020), and the *MuMIn* R package (Multi-model Inference, Bartoń, 2022). Sets of multiple linear regression models were fit to the data and ranked using the Akaike Information Criterion (AIC, Akaike, 1973). Observed water height data were obtained from NOAA Tide Station 8665530 (Charleston, SC). These data were reported at six-minute intervals; monitoring interval summaries were created by summarizing these six-minute increments across the monitoring periods. Wind data were obtained from the NOAA National Data Buoy Center (NDBC) Station FBIS1 on Folly Island, SC. These data were reported at 10-minute intervals and were also summarized by monitoring period. Additionally, hourly summaries were used to characterize wind and tide data together, to account for the differences in reporting frequencies. These hourly summaries were then used to create summaries at the time scale of reporting periods. From observation it was evident that different portions of the shoreline behaved differently over the monitoring period. Therefore, analyses were conducted separately on four distinct shoreline regions (*i.e.,* North, East, South, and West). For each of the four regions of the island, a global model was created with the average EPR for each monitoring period as the response variable, and the following predictor variables:

-number of intervals with wind > 20mph;
-number of intervals with tidal height > 1m NAVD88;
-number of intervals with both wind > 20mph and tidal height > 1m NAVD88;
-maximum tidal height during the monitoring period;
-maximum wind speed during the monitoring period;
-duration of monitoring periods in days.

This global model was then compared, using AIC values, to subsets of models including all possible combinations of predictor variables. The best model(s) for each region was identified as the model with the lowest AIC value. If the difference between model AIC values were less than two, the models were considered to perform equally well.

Elevation profiles

The GNSS was used to collect elevation data along five transects spanning the width of the island during the non-nesting period. Initial pre-construction transects were recorded on April 26, 2021, obtained from historical SCDNR monitoring. Because the reconstructed bank differed in shape significantly from the pre-existing bank, the transects were repositioned following construction and the new transects were used for all post-construction monitoring. Figure 4 shows the locations of the elevation transects. Nine points were recorded for each transect, at the highest ground point (HP) in the middle of the transect and then at high tide (HT), mid-tide (MT), low tide (LT) and subtidal (ST) points in both directions from the high ground point. All locations were initially chosen by observation on the day of monitoring to reflect existing conditions. Following the January 13, 2022 monitoring event, a decision was made to record the high point at the same location on all subsequent visits. The tide-line points were chosen by observation for all events. The rationale for this approach was that locations were expected to change position over time. Transect data were examined graphically to explore changes. Because the high points were collected at fixed locations throughout most of the monitoring events, these points were graphically compared and summarized as an indication of high ground elevation change.

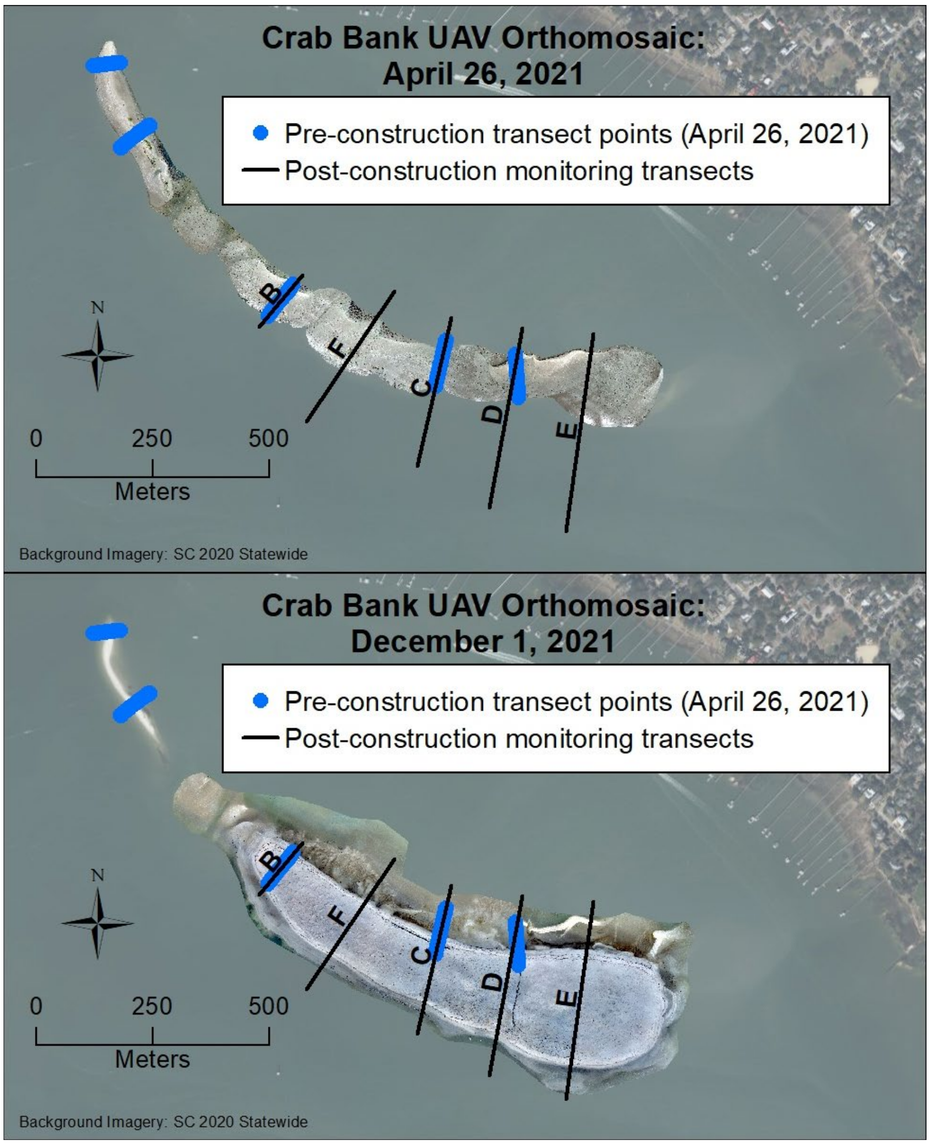

Figure 4. Location of elevation transect GNSS points (blue circles) recorded on Crab Bank pre-construction on April 26, 2021, and the locations of elevation transects (black lines) used to collect all subsequent elevation transect data. Top figure shows UAV pre-construction imagery of Crab Bank in April 2021, and the bottom pane shows UAV imagery from December 2021, immediately post-construction.

Sediment sample collection

Sediment samples were collected at each recorded elevation point using a push core (3.5 cm diameter x 10 cm depth) to characterize sediment composition. Sediment samples were placed in plastic bags and stored in a freezer (-10°C) until processed. Figure 5 shows an example of the locations of sediment samples collected on January 13, 2022.

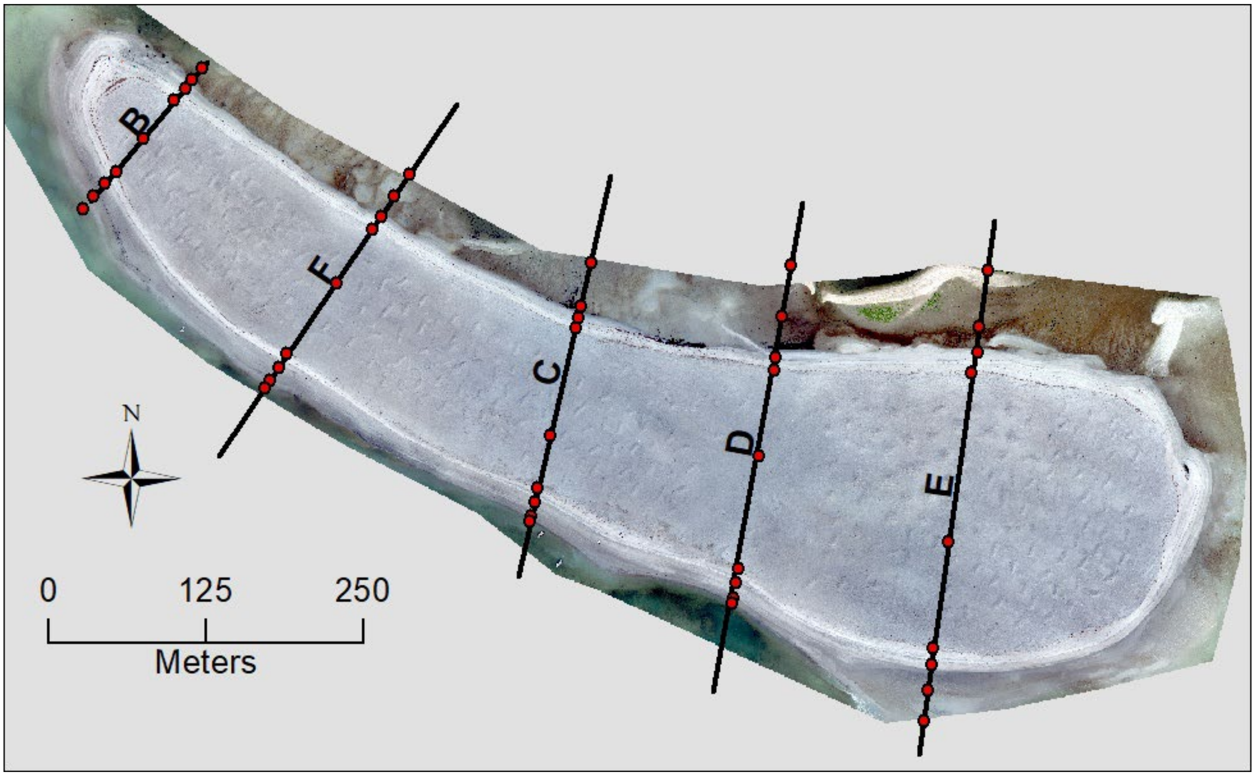

Figure 5. Example of the locations of sediment samples (red circles) collected on Crab Bank during monitoring events. Samples were collected at the observed high point as well as subtidally, and at the estimated low tide line, mid-tide line, and high tide line on each side of the island.

Sediment sample processing

Forty-five sediment samples were collected at each sampling event, but only a subset were used for analysis, and not every sampling event was analyzed. This initial analysis was conducted to explore general trends, with the additional samples being reserved if greater resolution (temporal or spatial) was warranted based upon the initial results. In the lab, 18-22 grams of the sample was analyzed for proportions (by weight) of sand (CaCO3 fraction removed, hereafter "sand"), silt and clay, and sand-sized calcium carbonate (hereafter "calcium carbonate" or $CaCO_3$) using procedures described in Folk (1980) and Pequegnat *et al.* (1981). Once proportional analysis was completed, the remaining materials were dry-sieved through thirteen 0.5-phi interval screens (-2.0 – +4.0; pebbles to silt, respectively) using a Ro-Tap® mechanical shaker. Grain size diameter (in millimeters) was determined by using the Udden-Wentworth Phi classification (Brown and McLachlan, 1990) and mean grain size (φ) was calculated using the following equation:

$$\Phi = -log_2(grain\ size\ diameter)$$

The samples were generally processed in batches of ten; one sample from each batch was randomly selected for Quality Assurance (QA) testing. QA samples were re-processed under blind conditions and results were compared to the original processing results. Differences between the original data and the QA data had to be $\leq$ 10% to pass. If a sample failed QA, the entire batch was re-processed. This procedure was continued until all batches passed QA.

Data were fit using generalized linear models and ANOVA with Tukey's HSD post hoc testing ($\alpha = .05$) was used to analyze changes over time for both proportions of grain type and mean grain size (phi). Grain size data were transformed to meet normality assumptions. Sand grain size was subtracted from 100 and then log transformed (log(100-sand)); calcium carbonate was fourth root transformed, and silt/clay grain size was log transformed. Analysis of change over time by sampling location used post-nourishment data only. Statistical analysis was conducted using JMP Software, R (R Core Team, 2022), RStudio (RStudio Team, 2020), and the R packages *agricolae* (de Mendiburu, 2021), *car* (Fox and Weisberg, 2019) and *dplyr* (Wickam *et al*., 2022).

Results and Discussion

Unoccupied aerial vehicle flights

A total of 12 flights were completed, one pre-construction and 11 post-construction. Overview maps of the digital orthomosaics and DSMs are provided in Appendix A. Crab Bank was initially monitored post-construction on December 1, 2021 (Figure 6) and approximately monthly thereafter except during the bird nesting season when monitoring occurred less frequently. Table 2 summarizes key UAV monitoring flight data. All flights resulted in products useful for visualizing the newly created island and for analyzing physical changes.

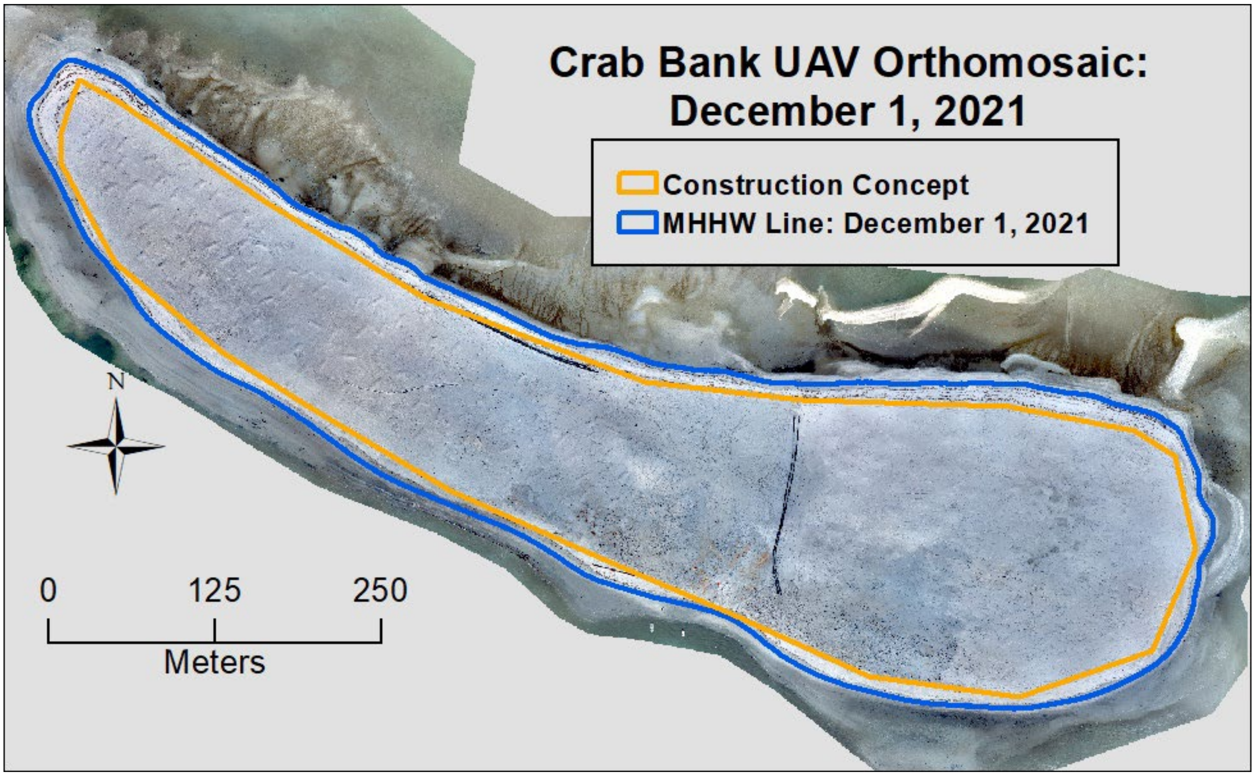

Figure 6. Initial post-construction UAV monitoring imagery of Crab Bank, created from imagery collected on December 1, 2021, showing the outline of the planned footprint (orange line) upon which construction was based, and the MHHW water polygon boundary (blue line) created from the DSM.

For those flights for which error was estimated (*i.e.,* when nesting birds were not present), estimated GNSS error ranged from 0.01 to 0.03 m horizontal and from 0.01 to 0.02 vertical (Table 3). RMSE of the final georectified products ranged from 0.02 to 0.06 m horizontal and from 0.03 to 0.09 m vertical (Table 3). These values fall within the range specified in the monitoring scope of work. The largest error was observed in the DSM for the February 14, 2022 flight (0.09 m) and in both the orthomosaic and DSM from the October 10, 2022 flight (0.06 m and 0.07 m, respectively). The cause of these higher georectification errors is unknown, but potentially resulted from slightly poorer image quality during these flights. The GNSS equipment remained highly accurate throughout all monitoring events, indicating that this equipment was unlikely to have caused increased error for any of the monitoring events.

Table 2. Key data for 12 UAV flights and resulting GIS products created during the monitoring of Crab Bank in Charleston Harbor, SC.

Flight Date	Altitude (m)	# GCPs	# Photos	Processed Area (ha)	Resolution (cm/pixel)
4/26/2021	61.0	16	866	29.7	1.7
12/1/2021	61.0	12	1,673	49.0	1.8
1/13/2022	61.0	16	1,312	45.8	1.8
2/14/2022	47.2	15	2,377	30.7	1.2
3/14/2022	68.6	14	1,084	33.5	1.9
4/25/2022	47.2	9	2,254	30.5	1.3
5/26/2022	47.2	9	2,313	29.5	1.3
7/25/2022	47.2	9	2,192	29.3	1.3
9/7/2022	47.2	9	2,368	30.1	1.3
10/10/2022	68.6	17	1,063	34.8	1.9
11/22/2022	68.6	13	1,138	36.2	1.9
12/19/2022	68.6	13	1,104	32.8	1.8

Table 3. Estimates of vertical and horizontal root mean square error for GNSS equipment and GIS products from monitoring UAV flights of Crab Bank in Charleston Harbor, SC. From April – September, 2022 error was not estimated because observed data were not collected on the island due to bird nesting.

Flight Date	Horizontal GNSS RMSE (m)	Vertical GNSS RMSE (m)	Horizontal Georectification RMSE (m)	Vertical Georectification RMSE (m)
4/26/2021	0.02	0.02	0.02	0.04
12/1/2021	0.02	0.01	0.03	0.04
1/13/2022	0.02	0.02	0.03	0.03
2/14/2022	0.02	0.02	0.04	0.09
3/14/2022	0.03	0.02	0.04	0.03
4/25/2022	N/A	N/A	N/A	N/A
5/26/2022	N/A	N/A	N/A	N/A
7/25/2022	N/A	N/A	N/A	N/A
9/7/2022	N/A	N/A	N/A	N/A
10/10/2022	0.01	0.01	0.06	0.07
11/22/2022	0.01	0.01	0.05	0.04
12/19/2022	0.03	0.02	0.04	0.04

<u>*Spatial analyses*</u>

Table 4 summarizes key morphological values calculated from the GIS products created from the UAV flights. The planar area enclosed within the MHHW contour polygon boundary immediately post-construction was 15.9 hectares (ha). This value remained stable over the course of the monitoring period, ranging from 15.8 to 16.1 ha, indicating that the area of habitat above MHHW remained nearly constant throughout the first year post-construction. It is noted that some areas within this footprint are expected to experience over-wash on extremely high tides and that the actual area of quality nesting habitat available is not equal the area above the MHHW line. The value is provided here as a relative index of stability. The width of the island, as measured across the MHHW polygon at fixed transect locations, remained relatively stable, with both net positive and negative changes in length among the five transects.

Table 4. Key morphological metrics for Crab Bank, in Charleston Harbor, SC, calculated from UAV-derived data collected during repeated post-construction monitoring visits. The MHHW footprint is the planar area within the MHHW contour created for each flight. Transect lengths are planar distance across the MHHW contour polygon along fixed transect lines (see Figure 4). Volume refers to the volume of material contained within the MHHW contour polygon.

		Transect Length (m)						
Flight Date	**MHHW Footprint (ha)**	**B**	**F**	**C**	**D**	**E**	**Volume (m^3)**	**Volume Change (m^3)**
4/26/2021	N/A	N/A	N/A	N/A	N/A	N/A	N/A	N/A
12/1/2021	15.9	93.4	140.4	148.9	179.1	243.2	157,409.28	N/A
1/13/2022	16.0	94.4	139.5	147.1	179.7	244.2	152,309.06	-5,100.22
2/14/2022	16.0	93.0	141.0	149.4	179.7	242.2	140,065.67	-12,243.39
3/14/2022	15.9	92.8	138.5	147.8	180.5	242.7	148,357.48	8,291.80
4/25/2022	15.9	93.2	137.5	148.7	181.2	242.8	146,517.53	-1,839.95
5/26/2022	15.9	90.5	136.6	150.7	183.0	242.8	146,315.80	-201.73
7/25/2022	16.0	88.2	137.1	151.8	183.4	243.2	146,391.96	76.16
9/7/2022	16.1	90.5	137.9	152.8	185.1	242.5	148,044.05	1,652.09
10/10/2022	15.8	85.8	131.7	148.9	182.2	239.5	141,005.93	-7,038.12
11/22/2022	16.0	89.2	137.1	152.4	185.0	240.2	145,121.66	4,115.73
12/19/2022	16.0	89.6	135.5	151.5	183.1	239.3	144,703.17	-418.49

Volume varied among monitoring events but showed a net loss over the monitoring period. Care is warranted when interpreting volumetric changes because relatively small errors of several centimeters in elevation can falsely indicate relatively large volume changes. Notably, the largest apparent changes in volume were associated with the largest estimated vertical georectification errors, which were estimated from the February 14 (0.09 cm RMSE) and October 10 (0.07 cm RMSE) flights (Table 3). A net loss of 12,706 m^3 was estimated between the December 2021 and the December 2022 flights, from products with estimated vertical georectification errors of 0.04 m (Table 3). This value is approximately 2.5 % of the volume of material originally placed on Crab Bank. In a worst-case scenario, a volume loss of this magnitude could erroneously be indicated from products with this level of error, although this is unlikely. While the observed data are strongly suggestive of a modest volume loss, the confidence around the estimated magnitude of this loss is low. Potential causes of volume losses include wind- or water-driven erosive forces and general substrate subsidence.

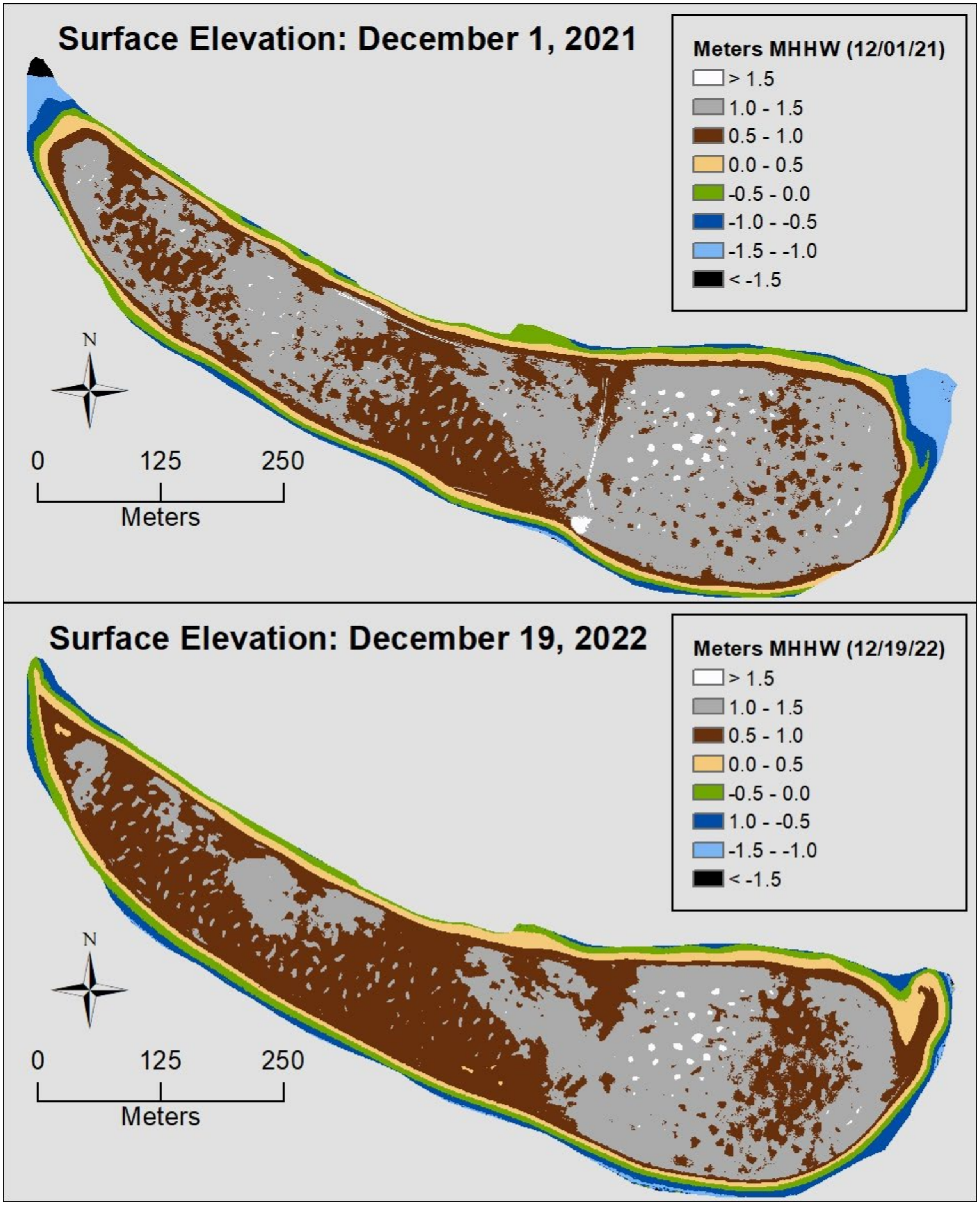

Figure 7. UAV-derived digital surface models (DSM) for Crab Bank created from imagery collected at the first post-construction monitoring event in December 2021 (top panel) and the final monitoring event in December 2022 (bottom panel). Elevation ranges have been symbolized in 0.5-m categories and shown relative to MHHW (0.8 m above 0 NAVD88, in Charleston Harbor).

Immediately post-construction and throughout the monitoring period most of the high ground surface of Crab Bank ranged from 0.5 m to 1.5 meters above MHHW (Figure 7). A pixel-level subtraction of the December 1, 2021 DSM from the final December 19, 2022 DSM indicated that the interior of the island experienced modest elevation losses (Figure 8). Within the interior of the island, the largest estimated losses ranged from 0.20 – 0.30 m. Larger changes, including both losses and gains of > 0.30 m, were observed on the southern border of the island and at the east and west ends of the island. The southern border became less sinuous over the monitoring period, with concave sections gaining elevation and convex sections losing elevation. Both ends of the island extended in length and gained elevation. The longest continuous area of loss was observed on the southeastern border. This smoothing of the southern boundary, combined with the elongating ends, is consistent with a general hypothesis of material redistribution driven by the prevailing longshore currents experienced on the shoreline.

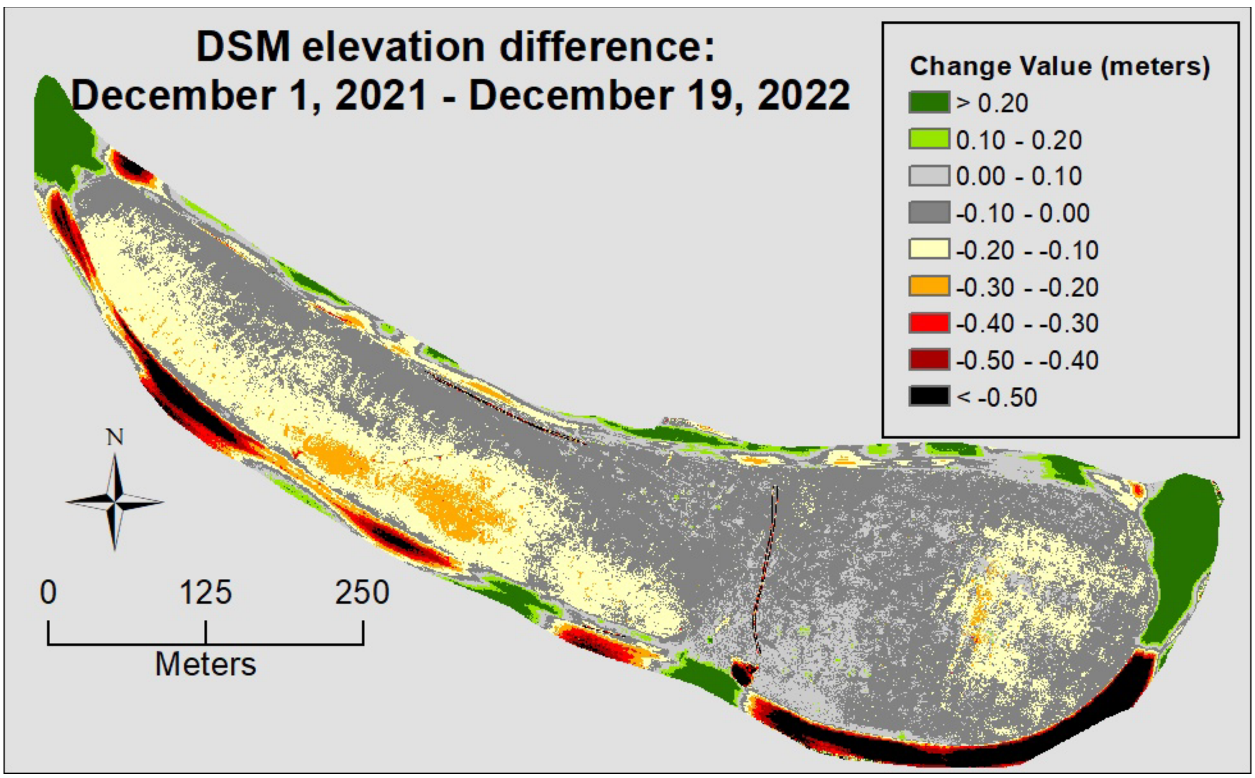

Figure 8. Pixel-level elevation differences between the DSM created from final post-construction monitoring event (December 2022) and the initial post-construction monitoring event (December 2021). The difference model was created by subtracting the initial DSM from the final DSM.

The risk of inundation of the high ground of Crab Bank was greatest in the central portion of the southern border and increased slightly over the course of the monitoring period. Although the MHHW water level was used as a meaningful datum for monitoring purposes, observed high tides regularly exceeded this value. This occurs by definition because the datum is a mean value, because onshore flow and local wind-driven waves cause higher than predicted water levels, and because mean sea level has increased since the datum was established based upon a 1983 – 2001 epoch. The highest observed water level of the post-construction monitoring period occurred on November 10, 2022 and was recorded as 0.786 m above MHHW on the Charleston gauge (NOAA Tide Station 8665530).

The potential for inundation on Crab Bank at this water level is shown in Figure 9 for the initial and final monitoring events. Due to estimated elevation losses, an area in the center of the island near the southern border was estimated to have a larger area at risk of inundation at this water level relative to the risk immediately post-construction. UAV imagery from before and after the observed high water event supports the likelihood that this area did, in fact, experience inundation in this time frame (Figure 10). A low area on the border of the island appears to have an erosion pattern typically caused by moving water, and high points within the potential inundation area had deposits of floating debris.

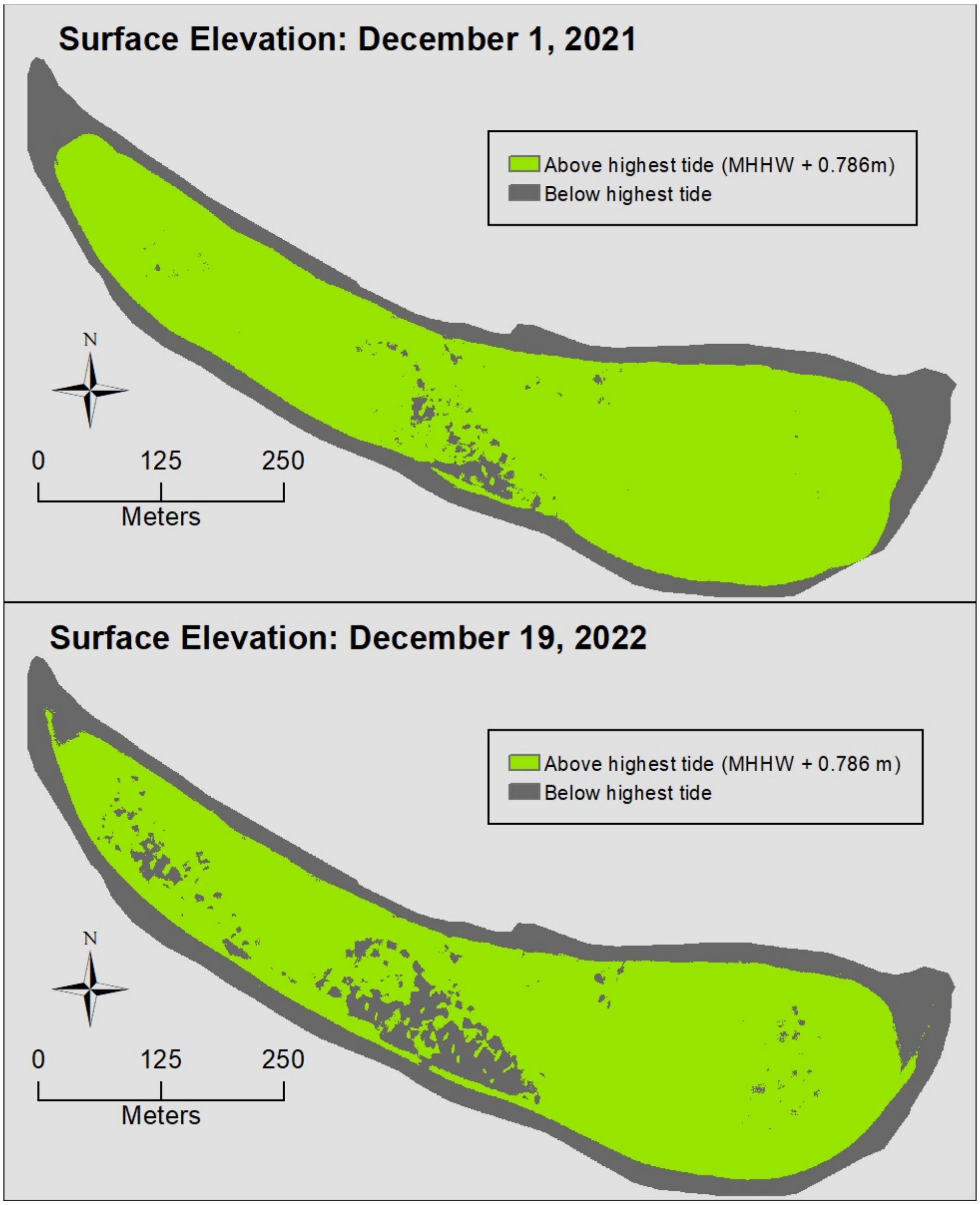

Figure 9. UAV-derived elevation of Crab Bank on December 1, 2021 and on December 19, 2022, symbolized to indicate areas above and below the observed highest observed water level during the period. The observed highest water level occurred on November 10, 2022 and was 0.786 m above MHHW (1.586 m above 0 NAVD88).

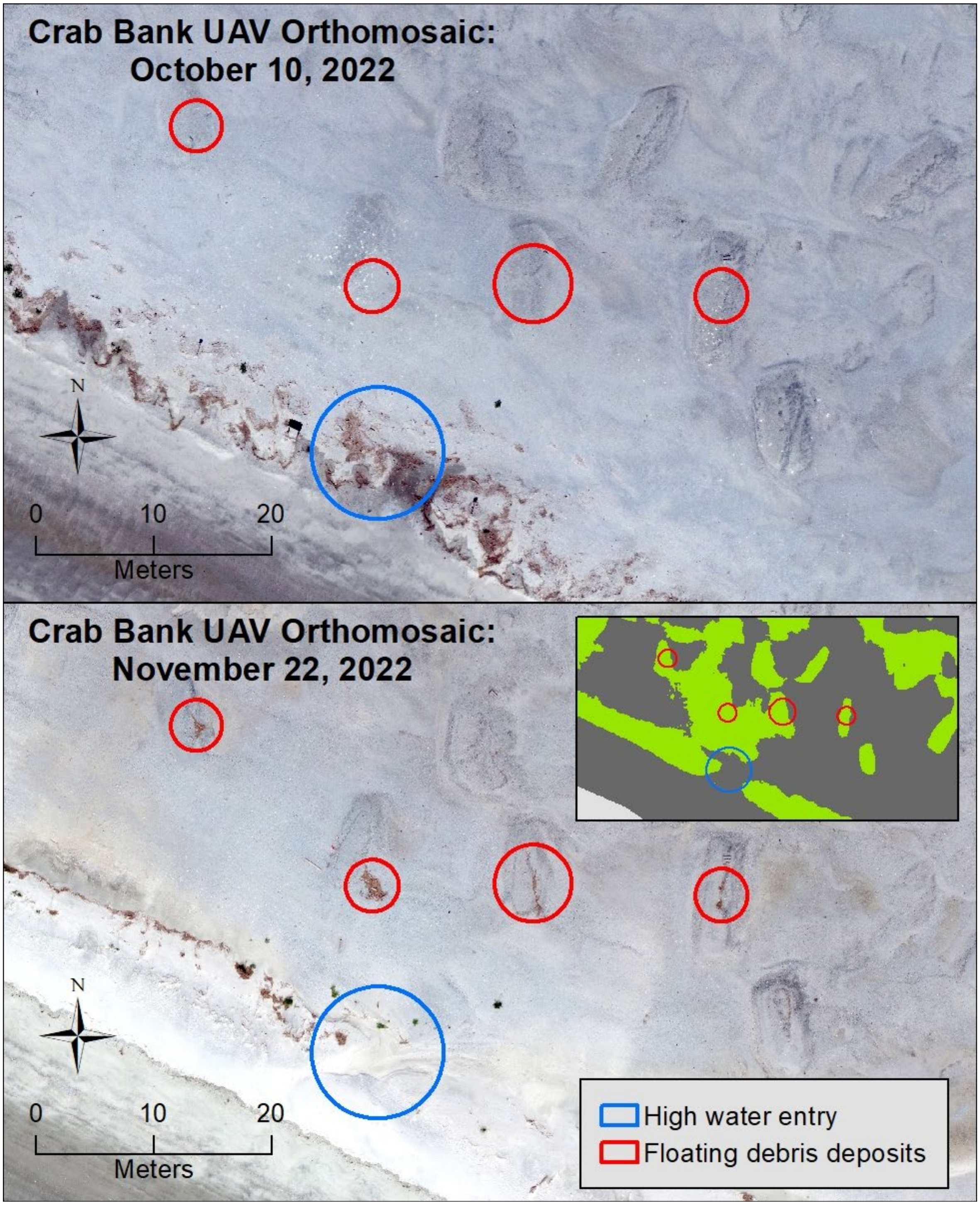

Figure 10. Detailed UAV imagery view of the Crab Bank southern shoreline on October 2022 (upper panel) and on November 2022 (lower panel), indicating evidence of local inundation between these monitoring events (circled features). The inset map on the lower panel shows the elevation of the view on November 22, symbolized to indicate areas below (gray) and above (green) the observed water level of November 10, 2022 which was the highest tide of 2022 at 0.786 m above MHHW. The November 2022 imagery shows an area of potential water ingress (blue circle) and floating debris deposits (red circles) that were absent in the October imagery.

Shoreline change analyses

Accuracy values assigned to shorelines used in the AMBUR analyses are shown in Table 5. Assigned accuracy ranged from 0.30 to 0.35 m for all flights for which error was empirically estimated. For flights during the bird nesting season, the assigned accuracy value was 0.50 m for all flights. The assignment of a large GNSS RMSE value to the bird season flights, and the addition of a large penalty to all shorelines, was done to ensure that the transect-level estimates of confidence for WLR values were conservative, given that all sources of error were not completely understood.

Table 5. Accuracy values used in AMBUR (Analyzing Moving Boundaries Using R) analyses of shorelines representing UAV-derived MHHW contours from imagery collected December 1, 2021 – December 19, 2022 on Crab Bank in Charleston Harbor, SC. Shaded values were not estimated directly, but were derived as described in the text.

Flight Date	Vertical GNSS RMSE (m)	Georectification RMSE (m)	Uncertainty Penalty	Total AMBUR Accuracy Value (m)
4/26/2021	N/A	N/A	N/A	N/A
12/1/2021	0.01	0.04	0.25	0.30
1/13/2022	0.02	0.03	0.25	0.30
2/14/2022	0.02	0.09	0.25	0.35
3/14/2022	0.02	0.03	0.25	0.30
4/25/2022	0.20	0.05	0.25	0.50
5/26/2022	0.20	0.05	0.25	0.50
7/25/2022	0.20	0.05	0.25	0.50
9/7/2022	0.20	0.05	0.25	0.50
10/10/2022	0.01	0.07	0.25	0.33
11/22/2022	0.01	0.04	0.25	0.30
12/19/2022	0.02	0.04	0.25	0.31

At the transect level, 169 of 241 transects had statistically significant ($p \leq 0.05$) WLR values (Figure 11). Both erosion and accretion were observed on the perimeter of Crab Bank, and observations supported findings of the width change analysis and the DSM subtractions previously described. When transect data were summarized by shoreline region, the southern shoreline had a mean negative rate of change (erosion) of -5.5 $m \cdot yr^{-1}$ (Table 6) and the other regions had net positive change rates, with both the east and west ends having large accretion rates. The northern shoreline had the smallest magnitude of change and remained relatively stable throughout the monitoring period. This finding is consistent with the observation of the smoothing of the southern boundary of the island, combined with the re-distribution of some materials to the east and west ends of the island.

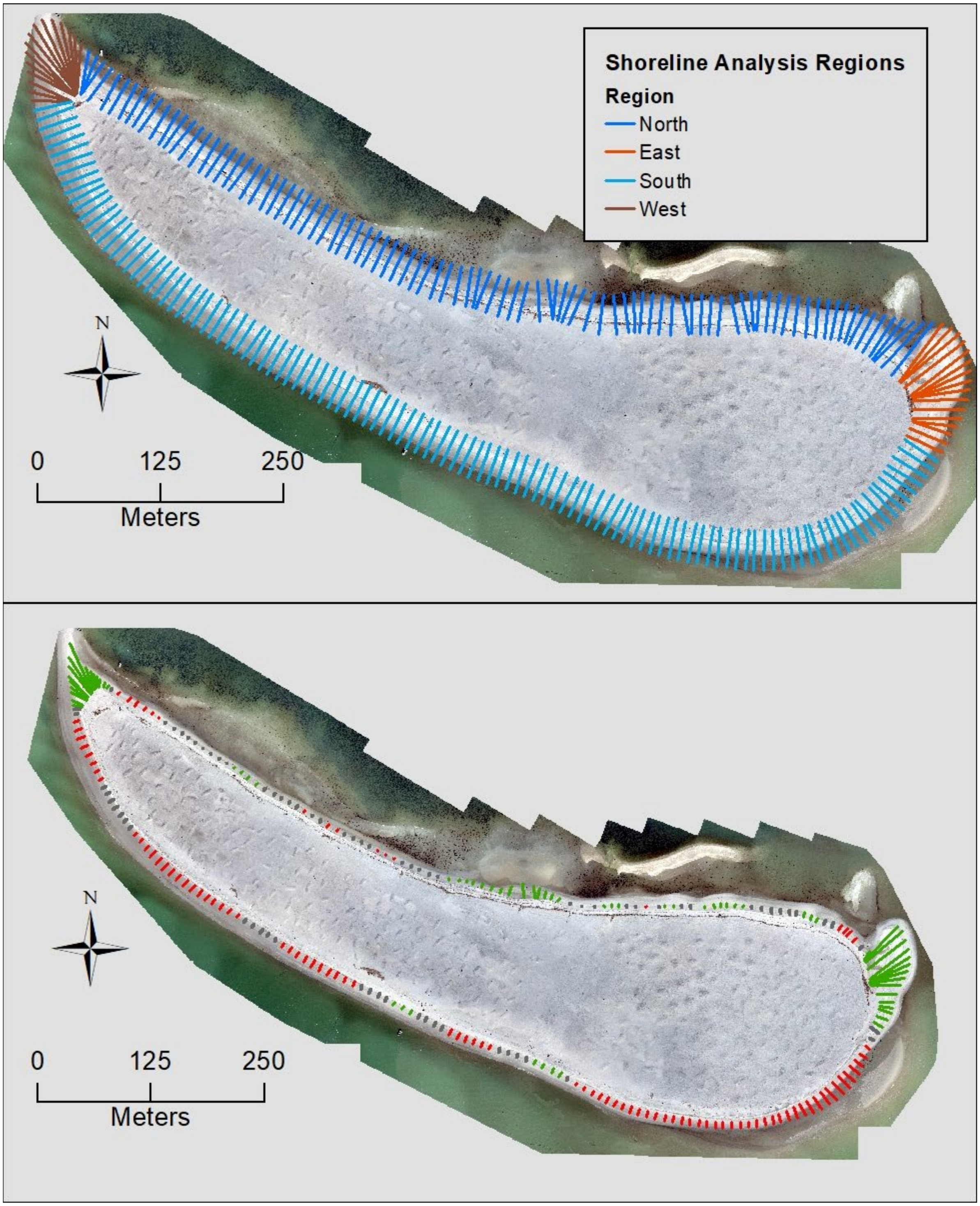

Figure 11. Upper panel: AMBUR analysis transects spaced at 10-m intervals on the Crab Bank shoreline. Colors correspond to regions of the shoreline that were used in the environmental analysis. Lower panel: Clipped transects with lengths corresponding the net shoreline change estimated using AMBUR software. For all transects with significant ($p \leq 0.05$) weighted linear regression rates (WLR), red lines indicate erosional transects and green lines indicate accretion transects. Non-significant transects are shown in gray. UAV imagery is from December 19, 2022.

Table 6. Mean weighted linear regression rates (WLR) of significant ($p \leq 0.05$) AMBUR-derived transects from four shoreline regions of Crab Bank in Charleston Harbor, SC, showing the number of transects (N) used to calculate each mean and the standard deviation of the mean in parentheses. Shoreline regions are shown in Figure 11.

Region	Mean WLR ($m \cdot yr^{-1}$)	N
North	1.5 (± 4.2)	51
East	30.6 (± 19.8)	16
South	-5.5 (± 4.4)	88
West	20.6 (± 13.9)	14

Environmental analyses

Multiple regression models using environmental observations to explain variation in AMBUR-derived EPRs for each time period were non-significant. Across all regions of the shoreline, null models were included in the best performing models when using AIC to evaluate model performance (Table 7). This suggests that the environmental predictors do not explain well the erosion patterns on Crab Bank. This could result from the juxtaposition of the granular environmental data (*i.e.,* reported on 6- and 10-minute increments for tide and wind, respectively) and the relatively coarse shoreline change rates (*i.e.,* a single rate for an entire 1-2 month period). The shoreline change rates are also confounded by general smoothing of the shoreline over time, which increased the variability of the EPRs within each region. On a very fine scale, this results in small areas of erosion and accretion in close proximity, but at a coarser scale, such as dividing the island into four portions, those signals become lost.

Table 7. Table of best performing models for explaining shoreline change rates for each of the four portions of the island, based on AIC values. In instances where differences in model AIC values were less than two, multiple models were considered to perform equally.

Section of Island	Predictor Variable(s) Included in Best Model	AIC Value	*P*-Value	R^2 Value
North	1. Max. wind speed, Intercept 2. Intercept	1. 59.3 2. 59.6	1. 0.062 2. 0.535	1. 0.29 2. 0
South	1. Intercept	1. 80.5	1. 0.158	1. 0
East	1. Intercept 2. Duration of monitoring periods, Intercept	1. 93.5 2. 94.7	1. 0.001 2. 0.128	1. 0 2. 0.17
West	1. Intercept 2. Number of periods with tidal height > 1m, Intercept 3. Duration of monitoring periods, Number of periods with tidal height above 1m, Intercept 4. Maximum tidal height, Intercept	1. 102.6 2. 102.9 3. 104.2 4. 104.3	1. 0.117 2. 0.086 3. 0.048 4. 0.164	1. 0 2. 0.24 3. 0.46 4. 0.13

An unconsidered factor likely influencing the erosional regime of the shoreline of Crab Bank is the vessel traffic in the adjacent shipping channel. This channel provides passage for large cargo ships and other vessels, which can generate significant wave energy. This wave energy was frequently observed by SCDNR researchers monitoring the island. Therefore, the lack of significance is not unexpected, given the short (*i.e.,* one year) time frame of this study, the inherent variability of the dependent and independent data, and the potential lack of key predictor variables in the analysis. Further refinement of this approach remains a potentially useful exercise to increase the understanding of factors driving the observed geomorphological changes on Crab Bank.

Elevation profiles

Cross-sectional GNSS elevation profile data were primarily collected in conjunction with sediment sampling and were not repeatedly collected at the same location for most stations. The initial plan to collect additional transect profile point data beyond the sediment sampling effort was altered because it was determined that, given the limits of staff time and equipment, it would be more productive to gather a dispersed set of elevation points to provide ground truthing for the UAV elevation data. As they were independent of tidal influences, however, the high points were collected repeatedly at the same locations for all monitoring visits from January through December, 2022 (Figure 12).

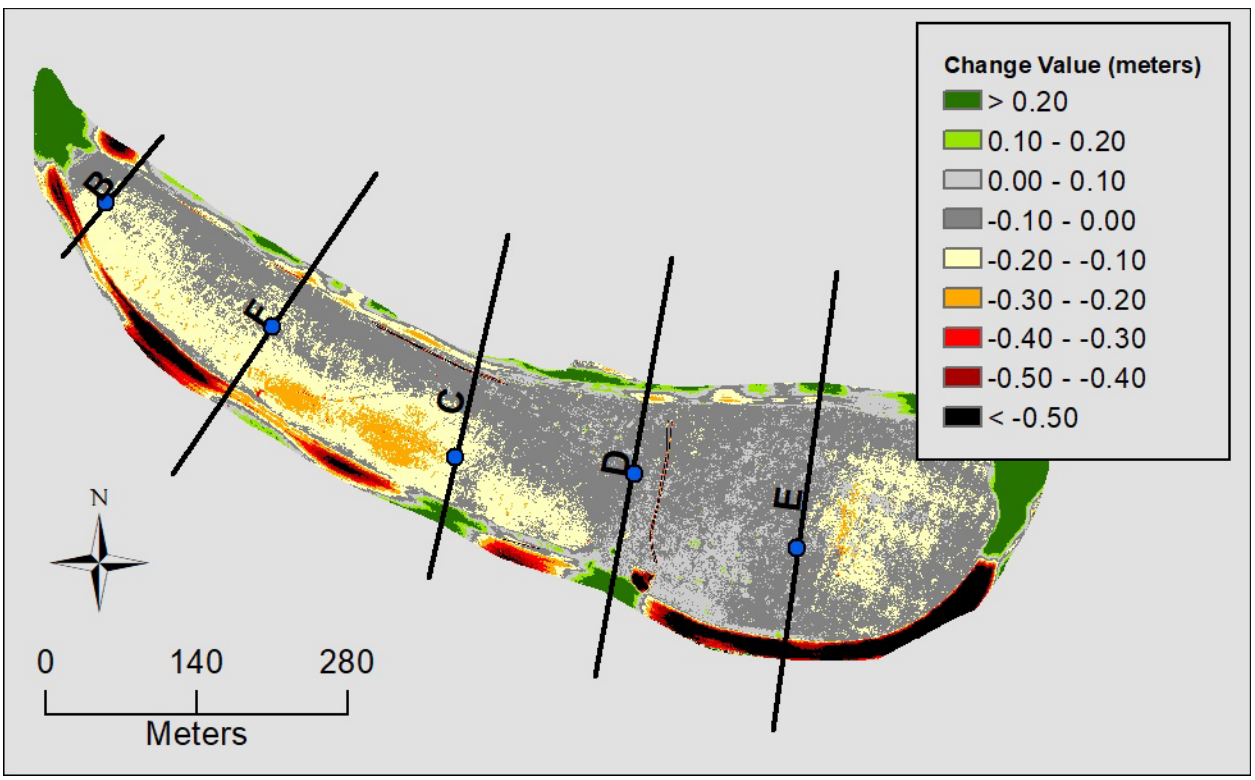

Figure 12. Location of repeated collections of high point GNSS elevation data from January 13 – December 2022, on Crab Bank, shown against a background of elevation change over the period. Black lines represent the transects where profile data were collected. For more information on the elevation change map see Figure 8. See Appendix B for raw profile information.

In most cases, the elevation at the point locations decreased over time with each successive monitoring visit, and in all cases there was a net decrease in elevation over the larger time frame (Figure 13). Because these data were independent of UAV-derived data, and because they were collected by a highly accurate GNSS, these results provide independent support for the elevation change estimated by UAV data (Figure 8). Although the precise magnitude of change is uncertain, it is evident that portions of Crab Bank experienced losses > 0.10 m in elevation over the monitoring period. Raw elevation profile graphs are provided in Appendix B.

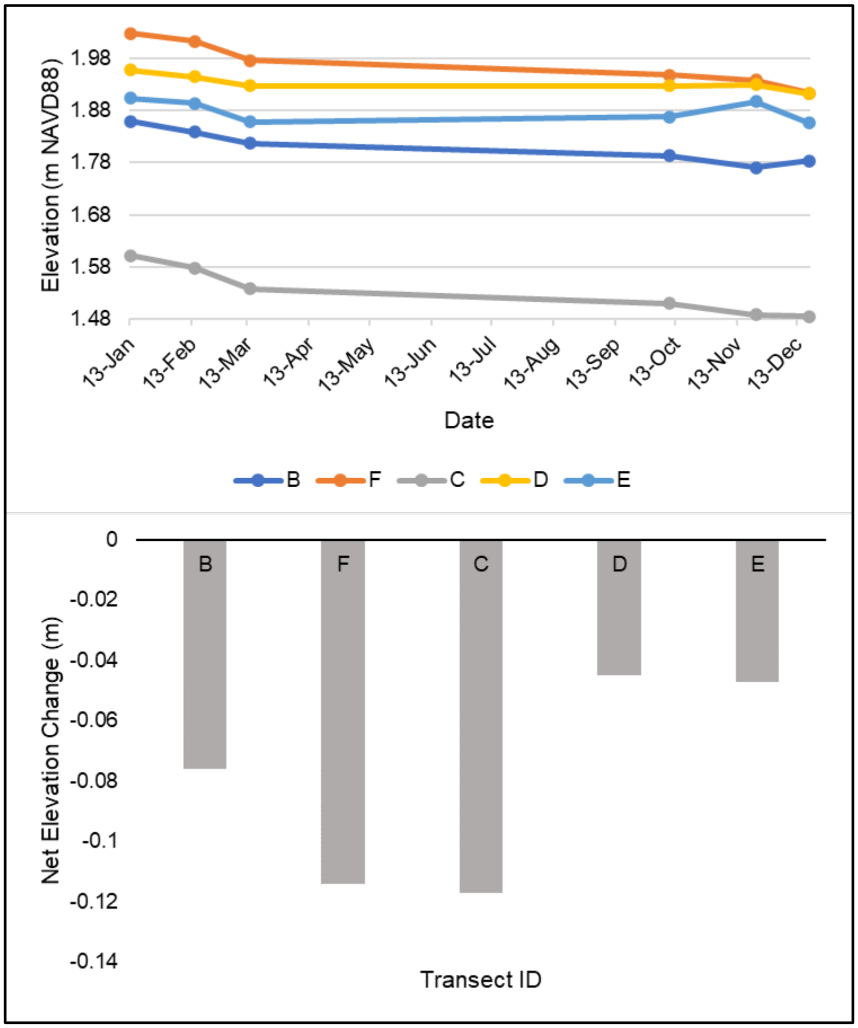

Figure 13. Change in GNSS elevation over time at repeatedly measured points on the Crab Bank (top panel) and net elevation change over the period (bottom panel).

Sediment sample analysis

Material collected in April 2021, pre-placement, was reasonably similar to that of the first post-placement collection in December 2021. Material collected in April 2021 contained finer sand (0.9 vs. 0.3 phi), but the December 2021 material contained a slightly higher silt/clay content (1.6 vs. 1.4 %). Neither difference was significant (p = 0.75 and 0.71, respectively). Overall, there was a significant decline in mean phi across the island over time (p < 0.0001). Variability in sand grain size increased significantly over time, but was lowest at high point sites, suggesting that variability is driven by mixing with existing materials rather than sorting of placement material (Table 8).

Table 8. Statistical results exploring differences over time and space for key sediment parameters. Letters indicate significant differences (LS Means A > B > C) identified in Tukey's *post hoc* tests. Strata codes are as follows: STW = subtidal west, MTW = mid-tide west, HP = high point, MTE = mid-tide east, and STE = subtidal east.

	Phi (Mean)	Phi (S.D.)	Silt/Clay %	$CaCO_3$ %
Adj. r^2	0.58	0.39	0.30	0.20
$F_{(model, error)}$	6.00 (27,72)	3.37 (27,72)	2.54 (27,72)	4.631 (7, 92)
p	<0.0001	<0.0001	0.0009	0.0002
Parameter *p* value				
TimePeriod	<0.0001	0.0063	0.0008	0.1035
ImmPost	A	B	A	
3moPost	B	AB	B	
10moPost	B	A	B	
12moPost	B	A	B	
Transect[Strata]	0.0110	0.0009	0.7835	
Strata	<0.0001	0.0005	<0.0001	0.0001
STW	B	ABC	B	BC
MTW	BC	AB	B	AB
HP	C	A	B	A
MTE	B	BC	B	AB
STE	A	C	A	C

In a series of samples collected following material placement, grain size patterns varied across the island, but both increasing sand and calcium carbonate and decreasing silt/clay percentages indicated a gradual coarsening of material between the December 2021 and December 2022 sampling events. Although the trends continued throughout the study period, the differences were only significant between the immediate post-placement and all other events (Table 8). Proportions of sand remained relatively unchanged over the course of the study (Figures 14). Calcium carbonate generally increased in proportion over time on the sides of the island (sub- and mid-tidal sites, Figure 15), however, there was no significant change across all post-placement time periods (p = 0.3287). Proportions of calcium carbonate increased with elevation and were significantly lower at sub-tidal levels than at the high point (Table 8). Silt and clay sediments were highest on the western side of the island pre-placement and were significantly higher on the eastern side immediately post-placement ($p < 0.001$) and remained generally higher on that side; however, silt and clay sediment percentages declined sharply throughout the remainder of the study (Figures 16, Table 8).

The large spike in silt/clay along the subtidal elevation on the eastern side immediately after the placement of material could be from the nourishment itself (perhaps the highest fine-sediment loads were deposited on that side first), or perhaps the eastern side of the island is the depositional side and finer sediments lost elsewhere on the island were carried over by tidal currents, or a combination of the two factors, among others. The high point sites remained relatively stable for all grain sizes throughout the study, showing little to no change pre- and post-nourishment (HP on Figures 14 - 16). Given the elevation of the high point sampling locations, the center of the island is not subjected to waves, boat wakes, or tidal currents. Changes to the sediment composition in the central portion of the island are likely wind- and rain-driven. These patterns are further supported by mean phi values declining (*i.e.,* coarsening) over the course of the monitoring at the sub- and mid-tide sites (except for the spike in silt/clay at subtidal east immediately after nourishment), and almost no change post-nourishment along the high point of the island. Raw sediment data are provided in Appendices C and D.

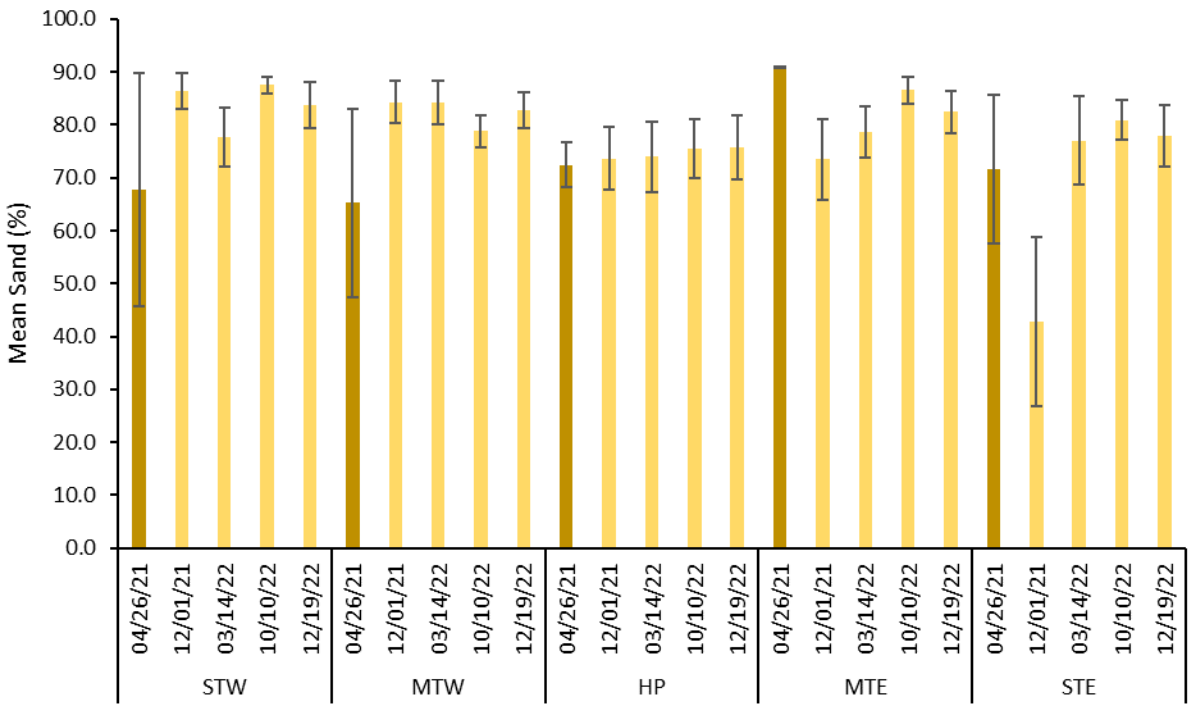

Figure 14. Average proportion of sand over time by sampling location (ST – Subtidal, MT- mid-tidal, HP- High Point, E – eastern side of island, W- western side of island) with standard error bars; darker shade indicates pre-nourishment data.

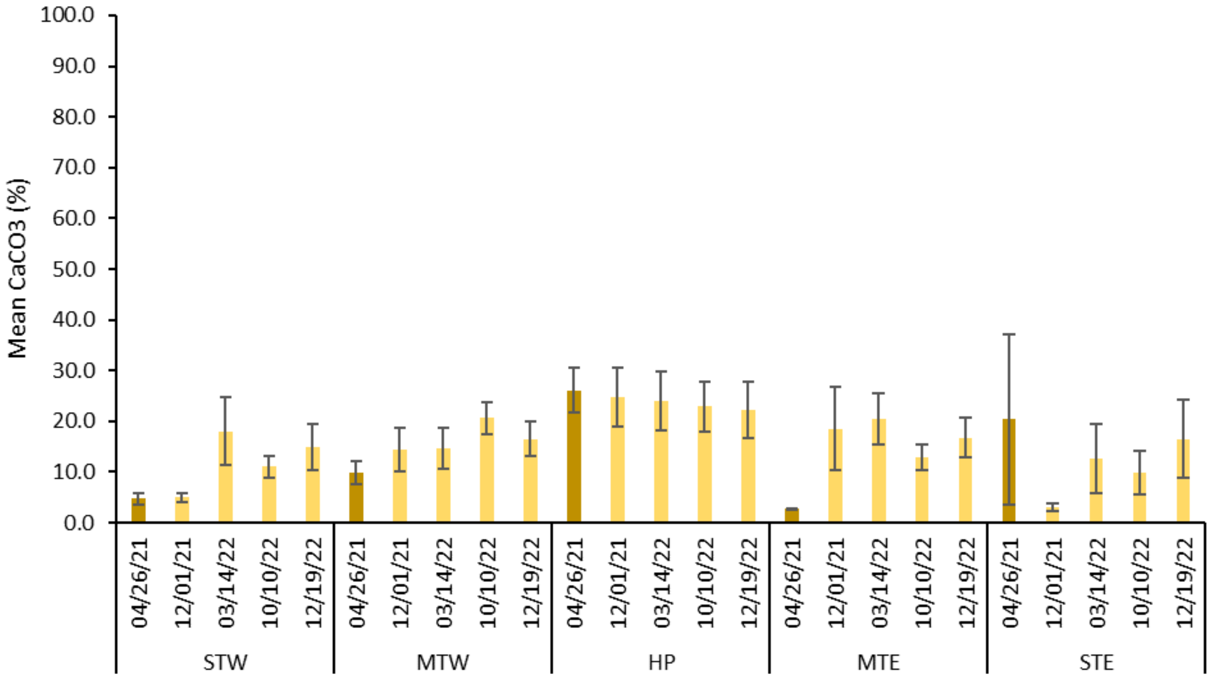

Figure 15. Average proportion of Calcium Carbonate ($CaCO_3$) over time by sampling location (ST – Subtidal, MT- mid-tidal, HP- High Point, E – eastern side of island, W- western side of island) with standard error bars; darker shade indicates pre-nourishment data.

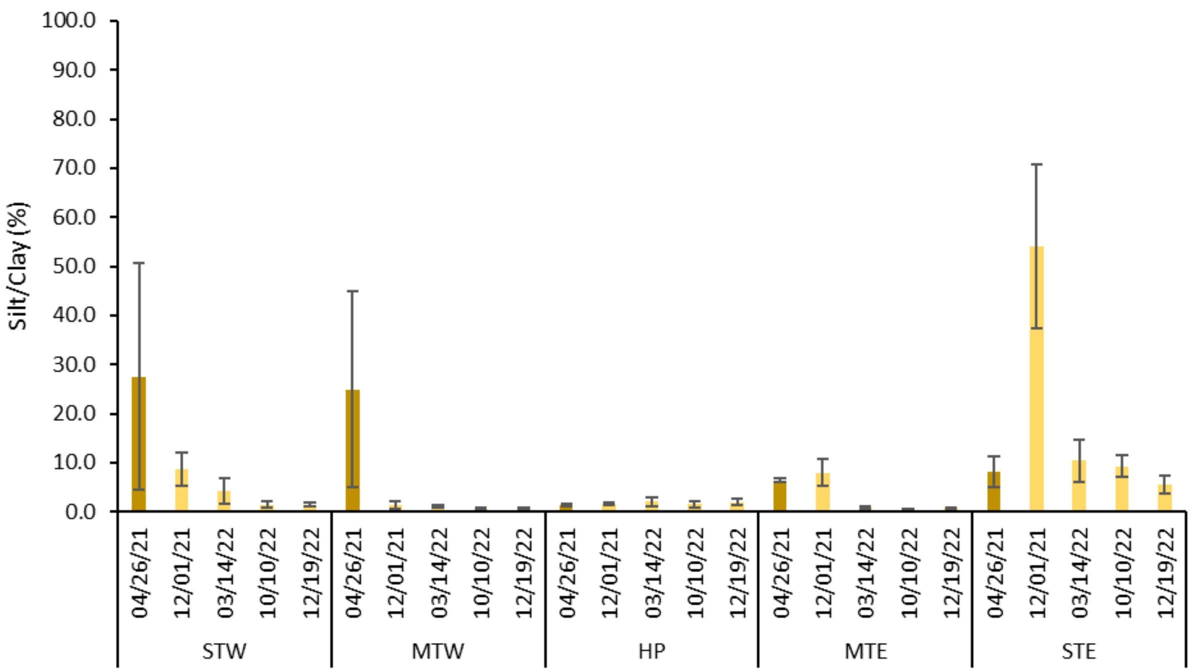

Figure 16. Average proportion of silt and clay over time by sampling location (ST – Subtidal, MT- mid-tidal, HP- High Point, E – eastern side of island, W- western side of island) with standard error bars; darker shade indicates pre-nourishment.

Literature Cited

Akaike, H. (1973). Information theory and an extension of the maximum likelihood principle. In: B. N. Petrov & F. Csáki (Eds.), *2nd International Symposium on Information Theory*, pp.267–281, Budapest, Hungary. Akadémia Kiadó.

Jackson, C. (2018). Analyzing Moving boundaries Using R – AMBUR. R package version 1.1.27 http://ambur.r-forge.r-project.org/.

Bartoń, K. (2022). MuMIn: Multi-Model Inference. R package version 1.47.1 https://CRAN.R-project.org/package=MuMIn.

de Mendiburu, F (2021). agricolae: Statistical Procedures for Agricultural Research. R package version 1.3-5, https://CRAN.R-project.org/package=agricolae

Fox, J. & Weisberg, S. (2019). An R Companion to Applied Regression, Third Ed. Thousand Oaks, CA: Sage. https://socialsciences.mcmaster.ca/jfox/Books/Companion/

Folk, R. L. (1980). *Petrology of sedimentary rocks*. Hemphill Publishing Company.

Pequegnat, W. E., Pequegnat, L. H., James, B. M., Kennedy, E. A. & Fay, R. R. (1981). Procedural guide for designation surveys of ocean dredged material disposal sites. Technical Report EL-81-1. Prepared for the U.S. Army Engineer Waterways Experiment Station, 286 pp.

R Core Team (2022). R: A language and environment for statistical computing. R Foundation for Statistical Computing, Vienna, Austria. https://www.R-project.org/

R Studio Team (2020). R Studio: Integrated Development for R. R Studio, PBC, Boston, MA http://www.rstudio.com/

Wickham, H., François, R., Henry, L. & Müller, K. (2022). dplyr: A Grammar of Data Manipulation. R package version 1.0.10, https://CRAN.R-project.org/package=dplyr